IEEE Access
Multidisciplinary | Rapid Review | Open Access Journal

Received 31 October 2023, accepted 18 November 2023, date of publication 28 November 2023,
date of current version 6 December 2023.

Digital Object Identifier 10.1109/ACCESS.2023.3337388

RESEARCH ARTICLE

Modeling of Extremely Short-Time Power Variations of Wound Rotor Induction Machines Wind Farms for Flicker Studies

SAEEDEH KETABIPOUR[1], HAIDAR SAMET[1], (Member, IEEE), MOHAMMAD MOHAMMADI[1], (Member, IEEE), QI LI[2,3], (Member, IEEE), AND VLADIMIR TERZIJA[4], (Fellow, IEEE)

[1]School of Electrical and Computer Engineering, Shiraz University, Shiraz 7134851154, Iran
[2]State Key Laboratory of Power Transmission Equipment and System Security and New Technology, Chongqing University, Chongqing 400044, China
[3]Electrical and Electronics Department, School of Engineering, The University of Manchester, M13 9PL Manchester, U.K.
[4]School of Engineering, Newcastle University, NE1 7RU Newcastle upon Tyne, U.K.

Corresponding authors: Haidar Samet (samet@shirazu.ac.ir) and Qi Li (qi.li@cqu.edu.cn)

This work was supported by the National Foreign Specialized Projects from the Chinese Ministry of Science and Technology under Grant DL2022165002L.

ABSTRACT Time-varying nature of wind farms is one of their major obstacles in providing a constant and reliable power output. They can be considered as a time-varying source of power considering different timeframes, from long to extremely short time periods. The focus of this study is modeling the wind farms for power quality studies by focusing on voltage flicker caused by the extremely fast wind farm output power variations. Despite there being several models developed for modeling the variations over longer time periods, there are few models that consider the extremely short time power variation, i.e., those in the range of 5-15 milliseconds. Our research started with the acquisition of a large data set of actual instantaneous voltage and current signals, recorded at a wind farm under different weather and operating conditions. The data set is utilized to develop practical models for the individual wind turbines and for the whole wind farm suitable for the mentioned extremely short time variations for the case of wind farms with the wound rotor induction generators (WRIG). The proposed model can be used for voltage flicker studies in power systems with WRIGs. The equivalent model of the WRIG is represented by a current source which its magnitude and phase change every half-cycle. It is observed that the variations of active and reactive powers follow a non-stationary seasonal time series where the seasonal part is not a simple single frequency. The seasonal term contains several frequencies which are modeled by 10 frequency components between 0.1 Hz to 1 Hz plus a DC component. The remaining component is modeled by autoregressive moving average (ARMA) models. The accuracy of the proposed equivalent model is assessed by several tests based on actual data and their corresponding simulated time series.

INDEX TERMS ARMA, extremely short-time variations, flicker, modeling, non-stationary, power quality, wind farms, wound rotor induction generators.

I. INTRODUCTION

A. MOTIVATION

To limit negative climate changes, to reduce dangerous environmental pollution, but also to develop and integrate sustainable generation, new measures have been recently undertaken to enable a massive integration of renewable energy sources throughout the world [1]. Therefore, the growth of the renewable energy technology as an alternative energy source, or as a complementary source of electricity generation, has been evidently significant. Wind energy is one of the most promising sources of green electricity generation. Studies showed that the percentage of installed capacities of wind turbines has been on the rise for almost consecutive years [2].

The associate editor coordinating the review of this manuscript and approving it for publication was Dinesh Kumar.

However, the renewable energy sources have some shortcomings. The stochastic nature of the wind power causes the output power changes in long, medium, short, and extremely short time periods, which has a big impact on the power system operation, planning, reliability, and power quality. The focus of this paper is the extremely short-time variations. This kind of power variation is caused due to stochastic variations in the wind velocity, wind shears, tower shadow, and yaw error [3]. The extremely short variations of the active and reactive powers cause voltage fluctuations, called voltage flicker [4]. Voltage flicker is a power quality problem that can be harmful to the sensitive electronic loads and can furthermore affect the performance of other types of loads. Wind speed is heavily dependent on weather conditions, geographic area, and seasons. Due to the importance of the subject so far, there have been many studies on modeling and analysis of uncertainties of wind energy and its variable nature [5]. Although many papers exist for studying the voltage flicker at wind farms, there are a very limited number of studies covering the abovementioned extremely short-term power variations. Such models can be used to generate data with similar characteristics to the actual data. Those data can be further used in voltage flicker studies in case of a lack of real data.

B. LITERATURE REVIEW

Time variations of the wind power and forecasting methods are divided into five major categories, based on the time intervals of wind speed changes.

The first group covers long-term forecasting methods, which usually include forecasting from one day to one week ahead and more. In [6], meteorological information is used to predict the wind power, which the relation between meteorological data and wind force is established based on the neural network. In [7], ten parameters of the main environmental data were collected from a region in southern Moldova, and based on the data, the numerical modeling of the vertical wind distribution were performed. Several neural network structures, such as neural networks with 1 or 2 hidden layers, have been employed to predict monthly average wind speed in Nigeria [8].

The second group contains forecasting methods in the mid-term time scale, which consists of the prediction for 6 hours to two days ahead. The mostly used methods in this time are based on neural networks and hybrid models, which are employed to predict the power and the speed of the wind [9], [10].

The third group covers many approaches, including short-term prediction methods with the forecasting 30 minutes to 6 hours ahead. For example, in [11], using a cluster analysis method, meteorological data are extracted for the use in neural network. Then it predicts wind power using a neural network in the short-term sense. A combination of support vector machines and an improved dragonfly algorithm for predicting short-term wind power changes is used in [12]. The improved dragonfly algorithm is used to select the optimal parameters of the support vector machine.

The fourth group includes very short-term forecasting methods, forecasting active power changes in the range of few seconds to 30 minutes ahead. For this time range, fewer articles are available. In [13], for prediction of wind speed in the time-range 1 s to 5 s ahead, an ARIMA linear model is implemented together with a filter which eliminates the undesired parts of the frequency spectrum of the measured wind speed. Also, in [14], a neural-fuzzy system was used to predict 2.5 minutes ahead of wind speeds and wind power in a region in Australia.

The fifth category, which is the major focus of this paper, includes the extremely short-term wind power changes prediction methods. It covers the forecasting for the extremely short-time active and reactive power variations for the time span of 0.01 s to 1 s. This type of models is suitable for power quality related studies, especially those related to voltage flicker and their impact to the system and other loads. In [15], the mechanical system of a wind turbine generator is modeled, and the wind speed fluctuations are modeled by a sinusoidal time-series with a frequency in the range of 0.01 Hz to 10 Hz. An analytical formula of the aerodynamic torque generated because of wind shear and tower shadow in a three-blade wind turbine is presented in [16]. A neural network-based model was proposed for wind turbine flicker calculations [17]. In [18], voltages and currents of the wind turbine are measured to calculate the flicker levels. Using the measured data of the instantaneous flicker, the short-term flicker is calculated. However, the models presented in [15], [16], [17], and [18] regarding the extremely short-term modeling are rather complex as they need many mechanical and electrical parameters of the systems. Also, some of the mentioned studies lack from utilizing the stochastic time series models which is the main character in the wind farms parameters variations. Furthermore, the previously utilized models for modeling the variations of wind power are stationary and do not represent the actual behavior of such variations. The frequency range of the wind farm output active and reactive power variations which causes flicker is 0.5-25 Hz. Hence, in the required model suitable for flicker studies the model parameters should be updated at least every 20 ms. In [19], [20], and [21], by forecasting the wind farm reactive power for half-cycle, i.e., 10 ms, ahead, the performance of the static VAr compensator in flicker mitigation is improved. In [22], ARMA models are used to model the extremely short time output active and reactive power variations for wind farms with squirrel cage induction generators (SCIG) wind turbines. It was shown that the actual and modeled data both result in almost similar power quality indices.

C. AIM AND SCOPE

Despite modeling of the extremely short time active and reactive power variations for SCIG wind farms, as presented in [22], a different variations behavior is observed for wind farms consisting of wound rotor induction generators (WRIGs) which will be analyzed in the present paper. The different dynamics comes from the different slip

controller in WRIG which allows a variable slip between 1% to 10% in contrast to SCIG where the slip varies only 1% [23]. The aim of the present paper is to derive a simple equivalent model for WRIG single wind turbines and WRIG wind farms that can be used for active and reactive power variations modeling that change every 10 ms. For this purpose, actual measurements of instantaneous voltage and current signals are collected at the Manjil wind power plant located in the north of Iran. Data collection was done both in summer and winter. One of the recorded active, P, and reactive, Q, powers are shown in Fig 1.

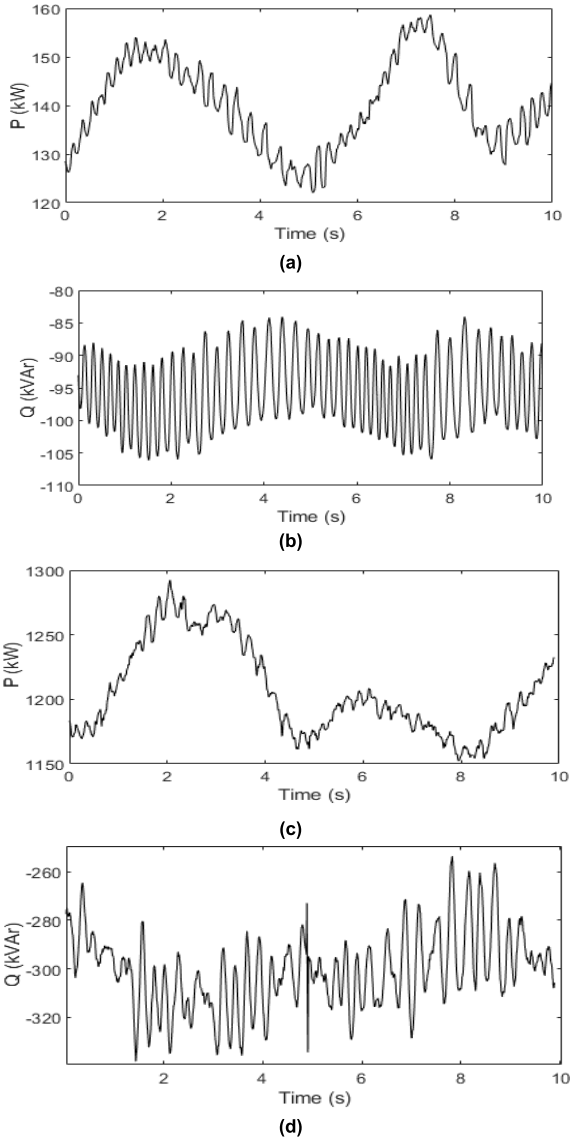

FIGURE 1. Active and reactive powers variations of an actual record (a) Turbine P (b) Turbine Q (c) Substation P (d) Substation Q.

As can be seen, the nature of changes of powers can be represented through a seasonal ARMA model. In seasonal ARMA models the mean of time series is changing over time. The remaining component after subtracting the seasonal term from the original time series can be treated as a simple ARMA model.

In the proposed model, the seasonal term is modeled as a multiple frequency oscillatory signal represented by a series of sinusoidal components. The coefficients of each sine component are estimated using the classical least-squares method. The remaining term is modeled through an autoregressive moving average (ARMA) process, what was justified by a strong stochastic behavior. Given that the recorded data were measured at different times and under different conditions, each data record has its own nature and its model parameters. There will be a set of sinusoidal and ARMA coefficients for every record. As a result, corresponding to every record, there will be a set of 21 parameters describing the low-frequency seasonal term and p+q+2 parameters determining the ARMA(p,q) model. The number of sinusoidal functions in the sinusoidal series is fixed for all records. However, records may have different ARMA order. Considering all the data records, there will be a database includes two matrices related to parameters describing seasonal mean (low frequency component) and the remaining ARMA term (high frequency compoment). At every run of the proposed model a row from the mentioned matrices which includes the model coefficients is selected randomly. It should be noted that based on the actual data, two types of non-stationary behavior are observed in the time series. First, they have a low-frequency time varying mean which is modeled here by a sinusoidal series. Second, the different records have different ARMA and sinusoidal model orders. In the next step, after obtaining the time series of active and reactive powers, the wind farm is modeled as a current source with changing magnitude and phase every 10 ms. The magnitude and phase of the current source are calculated based on the modeled active and reactive power series. The proposed model is verified by comparing the results of several applications for the actual and the modeled data.

D. CONTRIBUTION

Even though there are many studies for modeling time variations of wind speed and wind farm output powers (P and Q) in long-term, mid-term, short-term and very short-term, there is a need for further understanding of the same, but for the extremely short-term variations which are of the critical importance for understanding the voltage flicker caused by wind farms. As known, voltage flicker is one of attributes defining power quality at wind farms. We started our studies in this field by considering the basic models such as ARMA in [22] for wind farms based on SCIGs. In [22] simple ARMA models were utilized to model the active and reactive power variolizations. There, the seasonal changing mean didn't exist in the recorded time series. The study is continued in the present paper by focusing on wind farms with WRIGs. This type of generator has a different nature of output powers and a modelling approach just based on an ARMA model would lead to inappropriate representation of the physical nature of changes of the output P and Q. To cope with this challenge

the simple ARMA model has been extended with the seasonal ARMA model as discussed above. In this paper, through a more realistic modelling approach a better representation of wind farm output power changes is achieved, opening new opportunities for flicker studies and power quality assessment at wind farms.

II. DESCRIPTION OF THE TURBINES AND WIND FARMS PRACTICAL MEASUREMENTS

Manjil wind power plant, built in 1992, is in the north of Iran. It is one of the largest and oldest power plants built in Iran, including 61 WRIG wind turbines rated at 660 kW and 47 squirrel cage induction generator wind turbines rated at 550 kW, 500 kW, and 330 kW, respectively. The focus of this paper is on the WRIG wind turbines.

In this paper, two models will be proposed: one for the individual single WRIG wind turbines and one for a substation feeds 18 WRIG wind turbines. Note although there are some other WRIG wind turbines which are fed from other substations, our records are gathered from the substation shown in Fig. 2. So, as it is shown in Fig. 2, the measurements take place at two points: 1) 150 records at the terminals of the individual turbines specified by ''Turbine measurement'', 2) 183 records at the 20 kV switchgear of specified by ''Substation measurement''. The 18 wind turbines are connected through two feeders to the substation. Actual instantaneous voltage and current signals were recorded with a length of 10 s and a 128 μs sampling time. Records are captured using a portable recorder shown in Figure 2.b with the high-performance transformer clamps, Pince C113 LCA 1000/1, which can capture instantaneous current and voltage [24]. The error of instantaneous current and voltage measurements is less than 0.3 %.

The active and reactive powers of each phase are calculated using the integration over a full 50 Hz cycle window, i.e., 20 ms. The integration window was updated every 10 ms – see (1) and (2) [25]. In other words, we have a sliding 20 ms data window, which is updated every 10 ms. A full data window (20 ms) has 156 samples, what corresponds to 78 samples per half data window (10 ms). The active and

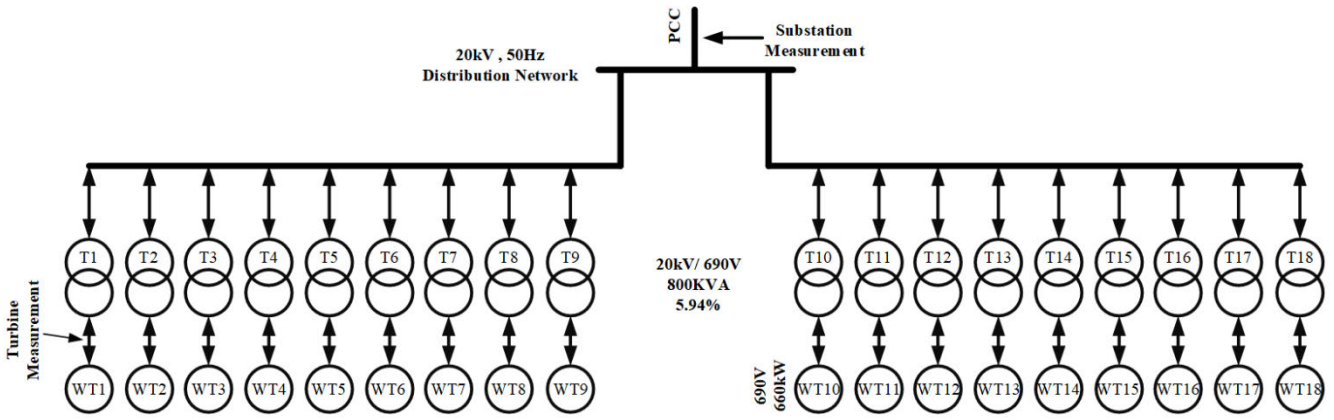

(a)

(b)

FIGURE 2. (a) The substation single-line diagram where the records are gathered. (b) The measurement device [24].

reactive powers were obtained as follows:

$$P(n) = \frac{1}{156} \sum_{k=78(n-1)+1}^{78(n+1)} v(k)\, i(k) \tag{1}$$

$$Q(n) = \frac{1}{156} \sum_{k=78(n-1)+1}^{78(n+1)} v(k-39)\, i(k)$$
$$k = 1, 2, \ldots, 78125 \quad \text{and} \quad n = 1, 2, \ldots, 1000. \tag{2}$$

The resulted P and Q in (1) and (2) can be considered as time series of active and reactive powers with a sampling time equal to 10 ms, what corresponds to 100 Hz. So, for a time duration of 10 s, every P and Q record can be considered a time series with total sample number equal to 1000. The sampling frequency is equal to 100 Hz which according to the Nyquist's theorem can covers frequencies up to 50 Hz in the P and Q time series. This is sufficient for flicker studies which need to cover frequencies up to 25 Hz. In the other side the total sample number of 1000 means that the resolution frequency of P and Q time series is equal to 50/(1000/2) = 0.1 Hz. So, the P and Q time series with total samples of 1000 and sampling time of 0.01 s can be decomposed to frequencies 0 to 50 Hz by frequency resolution equal to 0.1 Hz, i.e., f = 0, 0.1, …, 49.9, 50 Hz.

III. THE PROPOSED WRIG MODEL FOR FLICKER STUDIES

The actual recorded P and Q time series show two kinds of nonstationary behavior:

1) The first nonstationary behavior is due to the seasonal term of the time series. This kind of non-stationary behavior is observed even in short time durations such as 10 s. To be able to use the AMRA models, this term should be extracted and deduced from the original time series. It is observed that the extracted trend itself is not a simple single frequency component. It contains several frequencies which are modeled by 10 frequency components between 0.1 Hz to 1 Hz plus a DC component.
2) Although the remaining term presents a stationary ARMA process during the 10 s windows, it is non-stationary in long time periods. The reason is every actual record follows a different ARMA model which means the same ARMA model is not able to model the variations for the long time periods. This fact presents another type of nonstationary behavior in long time durations. Hence, different ARMA models are used for the different 10 s time windows in present paper.

The proposed WRIG model is presented in several stages. First is the extraction of the seasonal term from the active and reactive powers time series. Next, the seasonal term is modeled using the weighted sum of the sinusoidal functions. Then, modeling the remaining component by the ARMA models is described. After that, the coefficients databases are gathered and presented. Finally, the wind farm is equivalented as a variable current source.

A. EXTRACTION OF THE SEASONAL TERM

Through the actual records, it is observed that the active and reactive powers time series consist of a seasonal term. A moving data window with a length equal to 25 samples is used in (3) to extract the seasonal term (which is named low-frequency component, P_{LF}) from the main time series.

$$P_{LF}(n) = \begin{cases} \frac{1}{25} \sum_{k=n-24}^{n} P(k) & 25 \le n \\ \frac{1}{25} \sum_{k=1}^{25} P(k) & n < 25 \end{cases} \tag{3}$$

On the other hand, (4) is used to obtain the remaining term which is named high-frequency component:

$$P_{HF}(n) = P(n) - P_{LF}(n) \tag{4}$$

For example, for one of the actual data records, the high and low-frequency components of the wound rotor turbine active power are shown in Fig. 3. Note that in this section the focus is given to active power P, however, the same approach equally holds for reactive power Q.

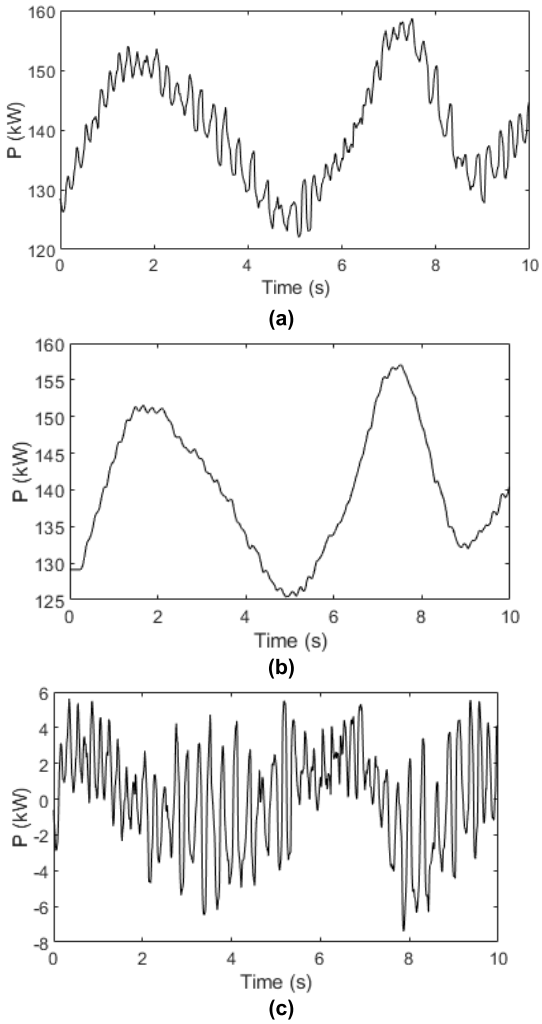

FIGURE 3. (a) The original wound rotor turbine active power time series (b) Low-frequency component (c) High-frequency component.

B. THE PROPOSED MODEL FOR THE SEASONAL TERM

It is observed that the low-frequency component contains frequencies between 0.1 Hz to 1 Hz. So, it is modeled as a distorted sine signal with the fundamental frequency of 0.1 Hz. In (5), there are 21 unknown coefficients, including DC component and 20 components related to frequencies in the range 0.1 to 1 Hz.

$$P_{LF}(n) = a_0 + \sum_{h=1}^{10} a_h \sin 2\pi h f_0 n\Delta t + b_h \cos 2\pi h f_0 n\Delta t \tag{5}$$

where $f_0 = 0.1Hz$, $\Delta t = 10ms$, and $n = 1, \ldots, 1000$.

Equation (5) has 21 unknown coefficients ($a_0, a_1, \ldots, a_{10}$, $b_1, \ldots, b_{10}$) and it can be written in the following matrix form:

$$\boldsymbol{A}\boldsymbol{x} = \boldsymbol{y} \tag{6}$$

where $\boldsymbol{x}$ is a 21×1 vector of unknowns, $\boldsymbol{A}$ is a 21×1000 matrix and $\boldsymbol{y}$ is a 1000×1 vector. They are presented as follows:

$$\boldsymbol{x} = \begin{bmatrix} a_0 \\ a_1 \\ b_1 \\ \vdots \\ a_{10} \\ b_{10} \end{bmatrix}$$

$$\boldsymbol{A}^T = \begin{bmatrix} 1 & \cdots & 1 \\ sin\,(0.002\pi) & \cdots & sin\,(0.002\pi * 1000) \\ cos(0.002\pi) & \cdots & cos\,(0.002\pi * 1000) \\ \vdots & \cdots & \vdots \\ sin\,(0.02\pi) & \cdots & sin\,(0.02\pi * 1000) \\ cos(0.02\pi) & \cdots & cos\,(0.02\pi * 1000) \end{bmatrix}$$

$$\boldsymbol{y} = \begin{bmatrix} \boldsymbol{P_{LF}}\,(\boldsymbol{1}) \\ \vdots \\ \boldsymbol{P_{LF}}\,(\boldsymbol{1000}) \end{bmatrix}$$

Using the least-squares method, the vector of unknowns $\boldsymbol{x}$ can be obtained as follows:

$$\boldsymbol{x} = \left(\boldsymbol{A}^T\boldsymbol{A}\right)^{-1}\boldsymbol{A}^T\boldsymbol{y} \tag{7}$$

The above estimation of the unknown vector with its coefficients was undertaken for all available data records. The obtained vectors $\boldsymbol{x}$ are used in the last algorithm stage for generating the simulated time series.

C. HIGH-FREQUENCY POWER VARIATIONS MODEL

The remaining term which contains the high-frequency component is modeled using ARMA models. ARMA models are widely used to model and predict a broad range of random phenomena [26], [27], but also wind power [28], [29]. An ARMA(s,r) process, can be expressed as follows:

$$\begin{aligned} P_{HF}(n) = {} & \varphi_1 P_{HF}(n-1) + \cdots + \varphi_s P_{HF}(n-s) \\ & + e(n) - \theta_1 e(n-1) - \cdots - \theta_q e(n-r) \end{aligned} \tag{8}$$

where $e(n)$ is the white noise with a zero mean and variance σ^2. The coefficients $\varphi_1, \ldots, \varphi_s, \theta_1, \ldots, \theta_r$ are the model parameters which can be determined for each data record. The model orders, s and r, are related to automatic regression (AR) and moving average (MA), respectively.

The best ARMA order for each time series is determined using the Schwartz test. First, a group of ARMA models for each record is selected as candidates, and then the best order is determined using the Schwartz test. In the Schwartz test, the model that minimizes (9) is selected as the best ARMA order.

$$SC(m) = \ln\sigma^2 + m(\ln N)/N \tag{9}$$

Here m is the total number of model parameters, and N is the time series length. This test is performed for all active and reactive powers time series regarding all records, and the best ARMA order is determined for each time series.

The best ARMA model and its coefficients of the high-frequency component are attained for the whole time series. The calculated ARMA coefficients will be used in the last stage for producing the non-stationary simulated time series.

D. THE COEFFICIENTS DATABASES

As mentioned in previous sub-sections, for every recorded data, the sinusoidal and ARMA coefficients related to the low and high-frequency components are calculated for all recorded time series. There are four kinds of time series in the present study 1) wind farm active power 2) wind farm reactive power 3) wind turbine active power and 4) wind turbine reactive power. Hence, there will be four databases corresponding to mentioned time series. The number of database rows for the first and second time series is 183 while it is 150 for the third and fourth time series which are equal to the number of the related actual records. Every row in the databases includes the corresponding sinusoidal and ARMA coefficients. If the maximum ARMA orders s and r in (8) are set to 12 then corresponding to every record there will be 12 AR coefficients (φ_1,…, φ_{12}), 12 MA coefficients (θ_1,…, θ_{12}), the mean value of the time series (M) and the standard deviation of the noise term (σ). So, in total, there will be 26 coefficients regarding the ARMA modeling of the high frequency component. The number of sinusoidal coefficients related to the low frequency component is 21. So, the columns number of the data bases is equal to 26+21 = 47. Hence, every row of the databases will be as follows:

$$[\varphi_1, \ldots, \varphi_{12}, \theta_1, \ldots, \theta_{12}, M, \sigma, a_0, a_1, \ldots, a_{10}, b_1, \ldots, b_{10}]$$

The data bases are included in the enclosed MATLAB codes which will be further illustrated in the Appendix.

At each model execution, randomly a row is selected. So, the proposed model can be considered as non-stationary. Different sets of the sinusoidal and ARMA coefficients will be chosen, and the time series will follow a different manner at every run. This behavior is like the real world, where the time series are non-stationary for long periods.

E. THE PROPOSED ELECTRICAL MODEL OF THE WRIG

As shown in Fig. 4, a current source with the changing magnitude and phase (every 10 ms) is used in the proposed model. The current source amplitude and phase ($I\angle\delta$) for every half-cycle are calculated by solving (10), which is the active and reactive powers balance in the circuit shown in Fig. 4(a).

$$\begin{cases} P(n) + RI(n)^2 = EI(n)cos(\delta(n)) \\ Q(n) + XI(n)^2 = -EI(n)sin(\delta(n)) \end{cases} \tag{10}$$

where $I(n)$ and $\delta(n)$ are the unknowns of (10) which are obtained by solving it for every half cycle n. $P(n)$ and $Q(n)$ are the wind farm powers in the n-th half cycle. R, E, and X are the Thevenin equivalent parameters.

The overall process is summarized in Fig. 4(b). First, a random integer number between one and the total number of records is generated. According to the generated number, a row is selected from the active and reactive coefficients database. Then the low and high-frequency components are generated based on the selected sinusoidal and ARMA coefficients sets. The time series are produced by adding low and high-frequency components together. In the last stage, the current source magnitude and phase are obtained by solving (10) at every half cycle.

F. MODEL SUMMERY

The inputs, outputs, and the internal variables of the proposed model are shown in a block diagram (see Fig. 5). The model inputs are the windfarm's size and the network Thevenin equivalent parameters (E, X, R). Inside the proposed model we have the coefficients data bases for generating P and Q time series which are calculated based on the actual records. At every run of the model a random row of these databases is chosen which contains 47 coefficients. In the next step the windfarm's size as one of the model inputs is used to update the coefficients values. The P and Q time series are generated in the next step and in the last step using the network Thevenin equivalent parameters (E, X, R) and by solving (10), the magnitude and angel of the current source are obtained.

IV. VALIDATION OF THE PROPOSED MODEL

In this section, several applications which require time series of active and reactive powers with extremely short time samples are utilized to evaluate the model accuracy. These tests are firstly applied to the actual measured data, then to the corresponding output data of the proposed model, and finally, the results are compared together.

A. POWER SPECTRAL DENSITY

The power spectral density (PSD) [30] is attained for all P and Q time series for the modeled and actual data time series according (11).

$$PSD_j(f) = \frac{1}{N \cdot f_s} \left| \sum_{n=1}^{N} P_j(n)\, e^{-i2\pi fn} \right|^2 \tag{11}$$

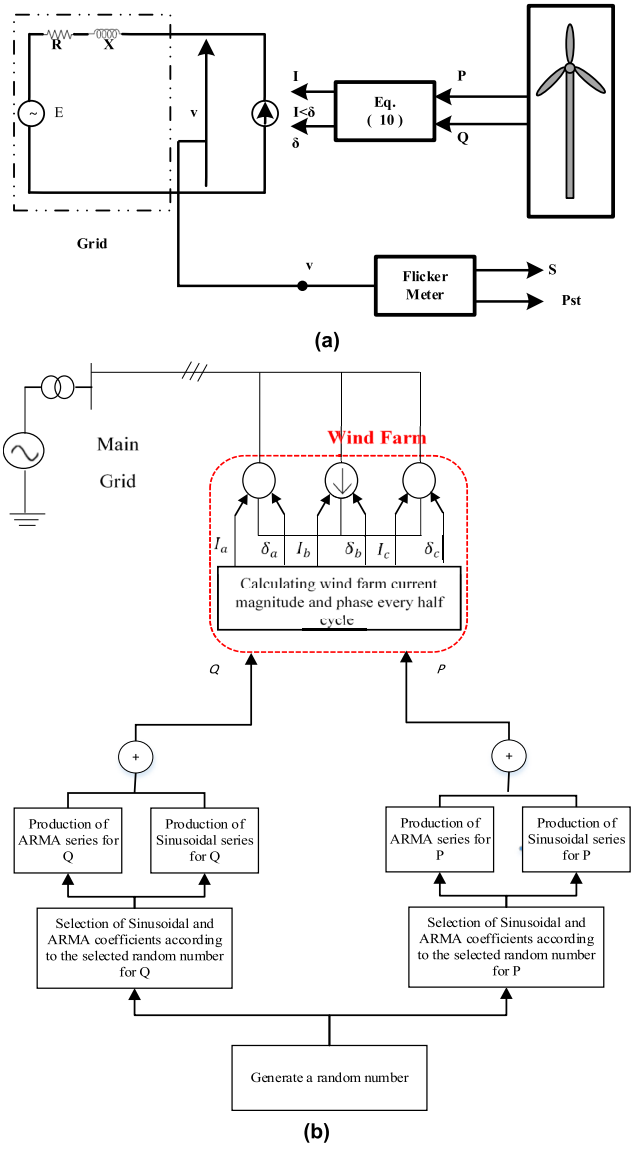

FIGURE 4. (a) A simple circuit for Equation 10 (b) The proposed electrical model.

$PSD_j(f)$ is the PSD at frequency f for jth record. The length of time series is N and equal to 1000 for the 10 s time series. f_s is the sampling frequency of the power time series. As the active and reactive powers time series are updated every 0.01 s, f_s is equal to 100 Hz. To cover all the recorded data, regarding every frequency (f), the mean of the PSD over all records, denoted as MPSD, is obtained as follows:

$$MPSD(f) = \frac{1}{J} \sum_{j=1}^{J} PSD_j(f) \tag{12}$$

where J is the number of data records.

The $MPSD$ is shown in Figures 6 and 7 belong to the single wound rotor turbines and the substation. Corresponding to every actual data simulated 20 time series of P and Q. The average PSD of the 20 simulated data is gathered, and it is averaged again by (12) based on all different records and compared with the MPSD of the actual data. The results show

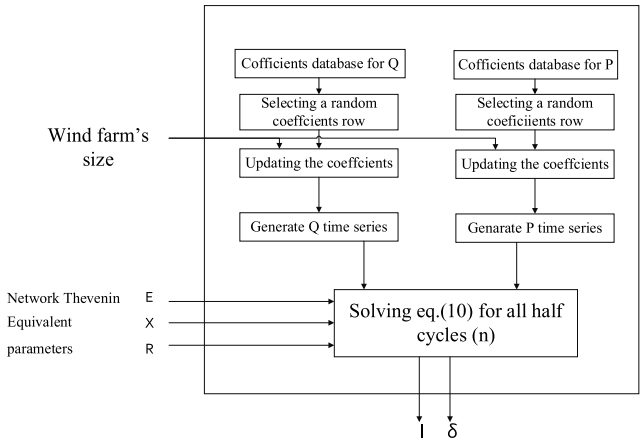

FIGURE 5. The block diagram of the inputs, outputs, and the internal variables of the proposed model.

that the *MPSD* of the simulated time series from the proposed model is close to the MPSD of the actual data.

B. INSTANTANEOUS FLICKER SENSATION

The proposed model main application is modeling the voltage flicker of the wind farms. As it is shown in Fig. 4(a), the flicker meter presented in IEC 868 [31] is used to calculate the instantaneous flicker sensation (S) of the turbine and wind farms corresponding to the actual and the modeled time series. The instantaneous flicker sensation related to a single wound rotor turbine and substation is shown in Fig. 8. The aim here is like the actual cases that at every recording, different data are gathered, at every run of the proposed models, different data are generated. Hence, the generated data are not same as the actual data, however both have same ARMA coefficients. This difference comes from the different noise term $e(n)$ of (8) in the actual data and the simulated data as at every run of the model a random noise term is used for $e(n)$ which generates different time series. Also, the start samples of P_{HF} (n) in (8) are different at every run of the model which is different from the actual records. In other words, unlike the forecasting studies where their aim is to forecast the exact values and fit the forecasted time series on the actual time series, here the aim is to generate time series where are totally different from the actual records but to have same characteristics to the actual data. Of course, different P and Q time series cause different instantaneous flicker sensation (S) signals. However, in calculating Pst in the next section, the samples magnitudes of S are important in flicker studies regardless of their time sequence. So, two S signals with different instantaneous values may result in equal values of P_{st}.

The short-circuit power of the network is equal to 200 MVA. According to Fig. 8, the average and maximum of S are in the same range for the actual and the corresponding modeled record which indicates using the modeled data produces a similar flicker level as the actual data.

Corresponding to every actual data, 20 time series of P and Q are simulated. Because of the random noise term, there will be 20 different simulated time series. The flicker indices for the 20 simulated time series are calculated and the average values are presented in Tables 1 and 2. Table 1 shows the mean instantaneous flicker of some actual records and their corresponding average of the 20 simulated time series. As it seen, the values obtained for the simulated records are close to the instantaneous flicker values of the actual data.

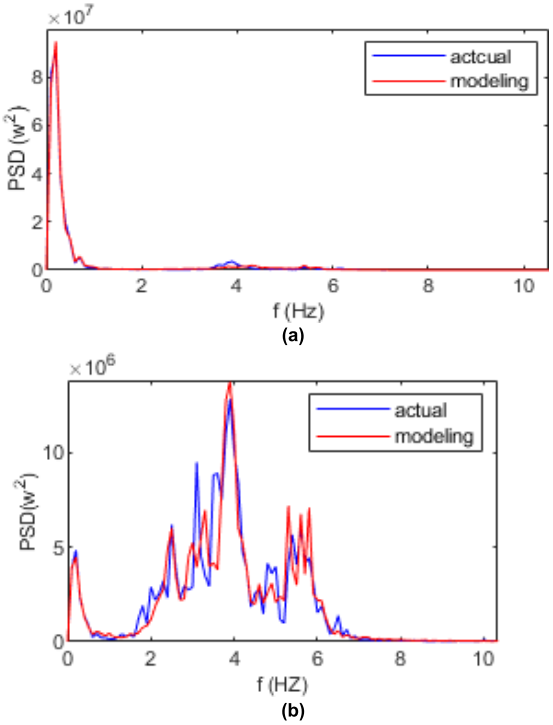

FIGURE 6. MPSD of the single turbines a) active power b) reactive power.

C. SHORT-TERM FLICKER (P_{st})

As the third test, the short-term flicker is computed considering the actual data and their corresponding simulations from the proposed model. Two different methods are utilized in this regard.

1) CALCULATION OF SHORT-TERM FLICKER ACCORDING TO IEC 868

Here, the P_{st} is calculated according to the IEC 868 standard, using the instantaneous flicker attained in the previous section. The values obtained for the short-term flicker of some actual records and their corresponding average of the 20 simulated time series are shown in Table 1. The values obtained for the P_{st} based on the actual records and their correspond output of the proposed model are close.

2) P_{st} APPROXIMATION BY THE MAXIMUM OF THE INSTANTANEOUS FLICKER

Here, the P_{st} is calculated by the maximum of the instantaneous flicker by (13) [32].

$$P_{st} = \sqrt{0.5096 * S_{max}} \tag{13}$$

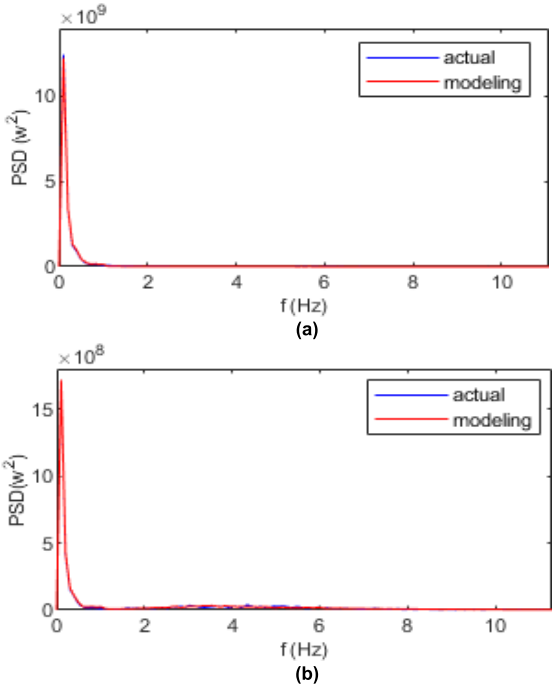

FIGURE 7. MPSD of the substation (a) active power (b) reactive power.

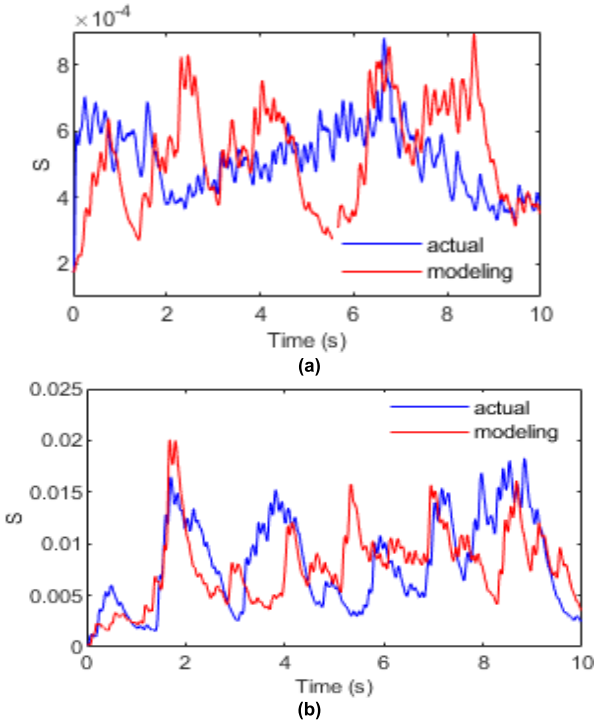

FIGURE 8. The instantaneous flicker sensation (S) (a) single turbine (b) the substation. As the noise signals are different for the actual and modeling data, S variations are not same. However, it doesn't matter as the average and maximum of S for the actual records are in same levels for the modeling.

where S_{max} is the maximum value of the instantaneous flicker sensation. The approximated P_{st} by (13) of some actual records and their corresponding average of the 20 simulated

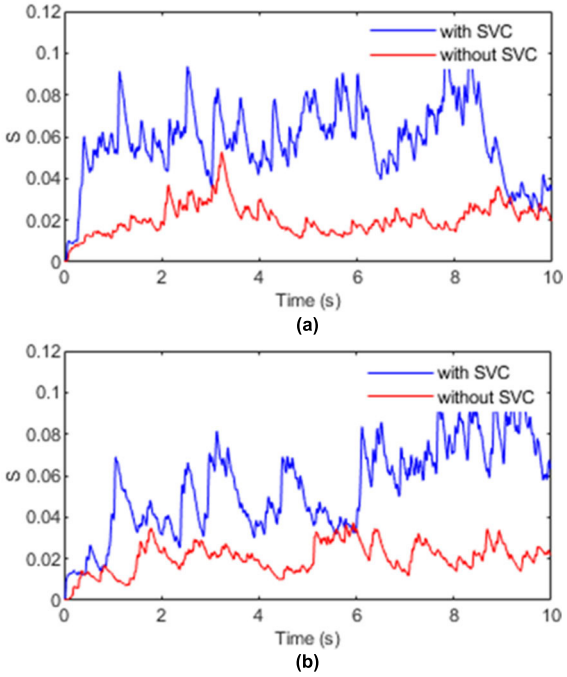

FIGURE 9. Evaluation of SVC impact on flicker mitigation a) using an actual record b) using the corresponding simulation from the proposed model.

time series are shown in Table 1. As can be seen in this test, the results of the actual and modeled records are similar.

D. CUMULATIVE P_{st}

The short term flicker resulted by the simultaneous operation of a set of wind turbines is called cumulative P_{st} ($P_{st,cum}$) and can be estimated using (14) [32].

$$P_{st,cum} = \sqrt[n]{\sum_{i=1}^{M} P_{st,i}^{n}} \tag{14}$$

where $P_{st,i}$ is the P_{st} produced by turbine i. M is the number of wind turbines, and n is the flicker summation factor. If the wind turbines have same rating, n is obtained by (15).

$$n = \frac{ln\,(M)}{\ln\,(P_{st\,cum}) - ln\,(P_{st\,ind})} \tag{15}$$

where P_{stind} is the short-term flicker when only a single turbine is operating.

Table 2 shows the values obtained for n according to some actual records and their corresponding average of the 20 simulated time series. It can be observed that the results of the actual records are close the modeling values.

E. VALIDATION OF THE PROPOSED MODEL IN EVALUATION OF THE COMPENSATOR PERFORMANCE

Here as another application of the proposed model, the performance of static VAr compensator (SVC) is evaluated using actual and modeled data. The voltage flicker is caused by the extremely short time variations of wind farm's active and reactive powers. SVC is relatively inexpensive equipment

TABLE 1. The flicker indices for single turbines and substation.

Mean values of the instantaneous flicker sensation for the actual and modelled records											
		Record 1	Record 2	Record 3	Record 4	Record 5	Record 6	Record 7	Record 8	Record 9	Record 10
Mean(s) turbine records	actual	0.00271	0.00266	0.00272	0.00084	0.00082	0.00085	0.00051	0.00052	0.00051	0.00029
	modelling	0.00262	0.00261	0.00259	0.00087	0.00083	0.00082	0.00050	0.00054	0.00052	0.00030
Mean(s) substation records	actual	0.00817	0.00798	0.00819	0.00915	0.00917	0.00943	0.00449	0.00441	0.00451	0.00488
	modelling	0.00782	0.00756	0.00802	0.00931	0.00875	0.00898	0.00465	0.00438	0.00444	0.00471
Short term flicker (Pst) for the actual and modelled records											
		Record 1	Record 2	Record 3	Record 4	Record 5	Record 6	Record 7	Record 8	Record 9	Record 10
Pst turbine records	actual	0.0427	0.0424	0.0430	0.0242	0.0239	0.0241	0.0180	0.0180	0.0181	0.0131
	modelling	0.0441	0.0449	0.0449	0.0259	0.0245	0.0254	0.0188	0.0194	0.0191	0.0133
Pst substation records	actual	0.0830	0.0830	0.0844	0.0860	0.0847	0.0859	0.0626	0.0626	0.0633	0.0615
	modelling	0.0882	0.0819	0.0832	0.0891	0.0871	0.0868	0.0661	0.0642	0.0681	0.0611
Approximated Pst by (13) for the actual and modelled records											
		Record 1	Record 2	Record 3	Record 4	Record 5	Record 6	Record 7	Record 8	Record 9	Record 10
Pst(max) turbine records	actual	0.0456	0.0451	0.0463	0.0275	0.0268	0.0272	0.0199	0.0196	0.0198	0.0139
	modelling	0.0491	0.0488	0.0481	0.0288	0.0276	0.0291	0.0208	0.0214	0.0209	0.0144
Pst (max) substation records	actual	0.0940	0.0948	0.0965	0.1033	0.0998	0.1021	0.0753	0.0745	0.0784	0.0754
	modelling	0.0991	0.0961	0.0982	0.1061	0.1022	0.1072	0.0801	0.0781	0.0801	0.0729

TABLE 2. Flicker summation factor (n).

Data type for s=50		Record 1	Record 2	Record 3	Record 4	Record 5	Record 6	Record 7	Record 8	Record 9	Record 10
Coefficient n turbine records	actual	1.6660	2.2367	2.5334	2.4500	1.9712	1.6543	1.9598	1.1489	1.1429	1.1392
	modeling	1.4991	2.3541	2.3891	2.6178	1.7291	1.8201	1.8981	1.1819	1.2001	1.2087
Coefficient n post records	actual	1.4384	1.4713	1.5848	2.2346	1.8250	1.9450	2.5425	0.3352	1.9749	2.7526
	modeling	1.5167	1.466	1.6342	1.9011	1.6891	2.0781	2.4687	0.3931	1.9211	2.5987

TABLE 3. SVC impact on the Pst a) without SVC (b) with SVC.

Data type for s=50		Record 1	Record 2	Record 3	Record 4	Record 5	Record 6	Record 7	Record 8	Record 9	Record 10
Pst Without SVC	actual	0.2024	0.2095	0.2130	0.2134	0.2065	0.2159	0.2126	0.2156	0.2017	0.2027
	modeling	0.2041	0.2111	0.2083	0.2176	0.2071	0.2187	0.2154	0.2149	0.2012	0.2061
pst With SVC	actual	0.1277	0.1361	0.1331	0.1452	0.1464	0.1461	0.1235	0.1322	0.1117	0.1077
	modeling	0.1265	0.1345	0.1325	0.1439	0.1441	0.1432	0.1201	0.1301	0.1166	0.1133

utilized to compensate the variations of reactive power and mitigate the voltage flicker [33]. SVC is installed in parallel with wind farm. At every half cycle it injects a reactive power equal to windfarm's reactive power but in the opposite direction. By this way in ideal case the summation of windfarm and SVC reactive power becomes zero. However, due to delays brought on both the reactive power calculation unit and the SVC's triggering fire angle, SVCs are unable to fully adjust for the rapidly varying reactive power. Hence, SVC by reducing the net reactive power that flows to the upstream network, can reduce the voltage flicker. The compensation of the reactive power is essential in wind and solar fields to mitigate their adverse impacts on the grid [34], [35]. There are currently wind farms where SVC is installed and in operation [36]. The impact of SVC on reducing the wind farms voltage flicker is studied here using the actual and modeled records. For this, the produced flicker by the wind farm is evaluated for two cases without SVC and with the SVC. The results of the two mentioned cases are presented in Fig. 9. Also, the Pst is provided in Table 3 for ten actual and modeled

records with and without the SVC. The results of the actual data are close to the results of the modeled data and show the accuracy of the above method.

V. CONCLUSION

In this paper, active and reactive powers extremely fast time variations for a wind farm and single wind turbines based on the wound rotor induction generators are modeled. It is observed that the variations follow seasonal time series. The seasonal term is modeled by a sinusoidal series that contains 10 frequencies from 0.1 Hz to 1 Hz beside the DC component. The remaining component is modeled by ARMA models. The sinusoidal series and ARMA models' coefficients are varying at every model execution so, the model can be considered non-stationary. A current source with changing magnitude and phase every 10 ms is utilized as the proposed model. The results are compared and validated based on a large set of actual records of instantaneous voltage and current signals. The actual records; 150 records of the individual turbines and 183 records at the 20 kV switchgear are used in 1) model creation and 2) model validation steps. In the first step, the actual data are used to create a large database for coefficients of the proposed model. Corresponding to every record there are 47 coefficients to create the active power time series and other 47 coefficients for the reactive power time series. In the second step, a large set of the actual data is utilized to validate the proposed models through several tests. The results of utilizing the actual data are compared with the results that came from the proposed models. The results are validated through 5 tests. As the proposed model is based on a large database of actual records, it can be considered as a comprehensive model which covers different weather and operation conditions. Results confirm that the proposed model has the ability for accurate modeling of the wind farm powers extremely fast variations.

APPENDIX

The proposed model is utilized through two MATLAB codes considering all the actual records. At every run of them, a set of sinusoidal and ARMA coefficients is randomly selected corresponding to an actual data record. Outputs are P, Q, delta, and I. Codes "swindturbin10s.m" and "swindfarm10s.m" are corresponding to the modeling of the single wind turbines and the wind farm, respectively.

REFERENCES

[1] M. G. Lobo and I. Sanchez, "Regional wind power forecasting based on smoothing techniques, with application to the Spanish peninsular system," *IEEE Trans. Power Syst.*, vol. 27, no. 4, pp. 1990–1997, Nov. 2012.

[2] *Renewables 2020: Analysis and forecast to 2025*. Accessed: 2020. [Online]. Available: https://iea.blob.core.windows.net/assets/1a24f1fe-c971-4c25-964a-57d0f31eb97b/Renewables_2020-PDF.pdf

[3] R. Fadaeinedjad, G. Moschopoulos, and M. Moallem, "The impact of tower shadow, yaw error, and wind shears on power quality in a wind-diesel system," *IEEE Trans. Energy Convers.*, vol. 24, no. 1, pp. 102–111, Jan. 2009.

[4] H. Al Riyami, A. Al Busaidi, A. Al Nadabi, M. Al Siyabi, O. H. Abdalla, K. Al Manthari, B. Hagenkort, S. Mirza, and R. Fahmi, "Power quality of Dhofar network with 50 MW wind farm connection," in *Proc. 18th Int. Middle East Power Syst. Conf. (MEPCON)*, Dec. 2016, pp. 33–39.

[5] L. Li, X. Wang, Q. Chen, and Y. Teng, "Dynamic equivalence method of wind farm considering the wind power forecast uncertainty," in *Proc. IEEE Innov. Smart Grid Technol.*, May 2019, pp. 1677–1682.

[6] S. Xiao, J. Lu, D. Li, H. Yu, M. Li, and J. Liu, "Long-term wind power forecasting model by multi meteorological variables based on data compensation," in *Proc. 2nd Int. Conf. Power Renew. Energy (ICPRE)*, Sep. 2017, pp. 451–455.

[7] V. Radulescu, "Selection of the main parameters for long term prediction of the atmospheric boundary layer in Romanian wind farms," in *Proc. Int. Symp. Fundamentals Electr. Eng. (ISFEE)*, Nov. 2018, pp. 1–6.

[8] D. A. Fadare, "The application of artificial neural networks to mapping of wind speed profile for energy application in Nigeria," *Appl. Energy*, vol. 87, no. 3, pp. 934–942, Mar. 2010.

[9] R. G. Kavasseri and K. Seetharaman, "Day-ahead wind speed forecasting using f-ARIMA models," *Renew. Energy*, vol. 34, no. 5, pp. 1388–1393, May 2009.

[10] S. Fan, J. R. Liao, R. Yokoyama, L. Chen, and W.-J. Lee, "Forecasting the wind generation using a two-stage network based on meteorological information," *IEEE Trans. Energy Convers.*, vol. 24, no. 2, pp. 474–482, Jun. 2009.

[11] A. Xu, T. Yang, J. Ji, Y. Gao, and C. Gu, "Application of cluster analysis in short-term wind power forecasting model," *J. Eng.*, vol. 2019, no. 9, pp. 5423–5426, Sep. 2019.

[12] L.-L. Li, X. Zhao, M.-L. Tseng, and R. R. Tan, "Short-term wind power forecasting based on support vector machine with improved dragonfly algorithm," *J. Cleaner Prod.*, vol. 242, Jan. 2020, Art. no. 118447.

[13] G. H. Riahy and M. Abedi, "Short term wind speed forecasting for wind turbine applications using linear prediction method," *Renew. Energy*, vol. 33, no. 1, pp. 35–41, Jan. 2008.

[14] C. W. Potter and M. Negnevitsky, "Very short-term wind forecasting for Tasmanian power generation," *IEEE Trans. Power Syst.*, vol. 21, no. 2, pp. 965–972, May 2006.

[15] O. Wasynczuk, D. Man, and J. Sullivan, "Dynamic behavior of a class of wind turbine generators during randon wind fluctuations," *IEEE Trans. Power App. Syst.*, vols. PAS–100, no. 6, pp. 2837–2845, Jun. 1981.

[16] D. Dolan and P. W. Lehn, "Simulation model of wind turbine 3p torque oscillations due to wind shear and tower shadow," in *Proc. IEEE PES Power Syst. Conf. Expo.*, Oct. 2006, pp. 2050–2057.

[17] S. A. Papathanassiou, S. J. Kiartzis, M. P. Papadopoulos, and A. G. Kladas, "Wind turbine flicker calculation using neural networks," *Wind Eng.*, vol. 24, no. 5, pp. 317–335, Sep. 2000.

[18] A. Larsson, "Flicker emission of wind turbines during continuous operation," *IEEE Power Eng. Rev.*, vol. 22, no. 2, p. 59, Feb. 2002.

[19] H. Samet and A. A. Bagheri, "Enhancement of SVC performance in flicker mitigation of wind farms," *IET Gener., Transmiss. Distrib.*, vol. 11, no. 15, pp. 3823–3834, Oct. 2017.

[20] H. Samet, S. Ketabipour, M. Afrasiabi, S. Afrasiabi, and M. Mohammadi, "Deep learning forecaster-based controller for SVC: Wind farm flicker mitigation," *IEEE Trans. Ind. Informat.*, vol. 18, no. 10, pp. 7030–7037, Oct. 2022.

[21] H. Samet, S. Ketabipour, and N. Vafamand, "EKF-based TS fuzzy prediction for eliminating the extremely fast reactive power variations in manjil wind farm," *Electric Power Syst. Res.*, vol. 199, Oct. 2021, Art. no. 107422.

[22] H. Samet, S. Ketabipour, and A. A. Bagheri, "Non stationary-ARMA flicker model for squirrel cage induction generators based wind farms," *IET Renew. Power Gener.*, vol. 15, no. 7, pp. 1542–1563, May 2021.

[23] *Vestas V47-660 kW Handbook*, Vestas Wind Syst., Denmark, U.K., 1997.

[24] *Portable Power Analyzer*. Accessed: 2023. [Online]. Available: http://behinehniroo.com/portable-power-analyzer-fault-recorder

[25] H. Samet, "Evaluation of digital metering methods used in protection and reactive power compensation of micro-grids," *Renew. Sustain. Energy Rev.*, vol. 62, pp. 260–279, Sep. 2016.

[26] P. Walker and O. Abdalla, "Discrete control of an AC turbogenerator by output feedback," *Proc. Inst. Elect. Eng.* , vol. 125, no. 10, pp. 1031–1038, Oct. 1978.

[27] O. H. Abdalla and P. A. W. Walker, "Identification and optimal output control of a laboratory power system," *IEE Proc. D Control Theory Appl.*, vol. 127, no. 6, pp. 237–244, 1980.

[28] H. Samet and F. Marzbani, "Quantizing the deterministic nonlinearity in wind speed time series," *Renew. Sustain. Energy Rev.*, vol. 39, pp. 1143–1154, Nov. 2014.

[29] H. Samet and M. Khorshidsavar, "Analytic time series load flow," *Renew. Sustain. Energy Rev.*, vol. 82, pp. 3886–3899, Feb. 2018.
[30] P. Stoica and R. L. Moses, *Spectral Analysis of Signals*. Upper Saddle River, NJ, USA: Prentice-Hall, May 2005.
[31] *Flickermeter-Functional and Design Specifications*," Standard IEC 868, IE Commission, 1986.
[32] P. P. Dutta, A. H. Fahad, and A. H. Chowdhury, "A comparative study of short term flicker severity due to electric arc furnace operation," in *Proc. 8th Int. Conf. Electr. Comput. Eng.*, Dec. 2014, pp. 647–650.
[33] F. Shojaei, H. Samet, and T. Ghanbari, "Filters optimized tuning for wind farms reactive power calculation," *IEEE Trans. Instrum. Meas.*, vol. 70, pp. 1–9, 2021.
[34] S. Ketabipour, H. Samet, and N. Vafamand, "TS fuzzy prediction-based SVC compensation of wind farms flicker: A dual-UKF approach," *CSEE J. Power Energy Syst.*, vol. 8, no. 6, pp. 1594–1602, Nov. 2022.
[35] H. Samet, S. Ketabipour, S. Afrasiabi, M. Afrasiabi, and M. Mohammadi, "Prediction of wind farm reactive power fast variations by adaptive one-dimensional convolutional neural network," *Comput. Electr. Eng.*, vol. 96, Dec. 2021, Art. no. 107480.
[36] *SVCs for Voltage Stabilization in Grid With Heavy Wind Power Penetration*. Accessed: 2010. [Online]. Available: https://library.e.abb.com/public/16200070bd7ac76c8325773b0028ade7/A02-0204%20E%20LR.pdf

SAEEDEH KETABIPOUR was born in Isfahan, Iran, in 1986. She received the B.Sc. degree from the Khuzestan Water and Electricity Industry Research and Educational Center, Ahvaz, Iran, in 2010, the M.Sc. degree from the Islamic Azad University of Khomeini Shahr, Isfahan, Iran, 2013, and the Ph.D. degree from Shiraz University, Shiraz, Iran, in 2022, all in electrical power engineering. Her main research interest includes the power quality of power systems.

HAIDAR SAMET (Member, IEEE) was born in Baghdad, Iraq, in 1978. He received the B.Sc. degree from the Isfahan University of Technology, Isfahan, Iran, in 2000, the M.Sc. degree from the Sharif University of Technology, Tehran, Iran, in 2002, and the Ph.D. degree from the Isfahan University of Technology, in 2008, all in electrical engineering. In 2008, he joined Shiraz University, Shiraz, Iran, as a Faculty Member, where he is currently a Professor of electrical engineering with the Department of Power and Control Engineering. His main research interest includes the application of DSP techniques in power systems, such as protection and power quality.

MOHAMMAD MOHAMMADI (Member, IEEE) received the B.Sc. degree from Shiraz University, Shiraz, Iran, in 2000, and the M.Sc. and Ph.D. degrees from the Amirkabir University of Technology, Tehran, Iran, in 2002 and 2008, respectively. He is currently a Professor with the Department of Power and Control Engineering, Shiraz University. His research interests include power system probabilistic analysis, power system security assessment, machine learning, and power system dynamic analysis.

QI LI (AKA STEVEN) (Member, IEEE) was born in Hunan, China, in September 1984. He received the B.Eng. degree in electrical and electronics engineering from the University of Birmingham and the Huazhong University of Science and Technology, in 2007, and the M.Sc. (Hons.) and Ph.D. degrees in electrical power engineering from The University of Manchester, in 2009 and 2013, respectively. Since then, he has been with The University of Manchester and National Grid, U.K., for six years, before joining Chongqing University, as a 100 Talents Plan Associate Professor of Chongqing City. Within academia and industry, he has led around 20 research projects with wide range of topics for power industry. His main research interests include electromagnetic environmental emissions from UHV/EHV transmission lines and the application of artificial intelligent into power systems. He is an Active Member of CIGRE working group B2.69, a Committee Member of IEEE PES Transmission and Distribution Satellite Committee, and a Youth Committee Member of China Electrotechnical Society. Acting as a main contributor, he has won twice the IET Innovation Awards (2012 and 2015).

VLADIMIR TERZIJA (Fellow, IEEE) was born in Donji Baraci (former Yugoslavia). He received the Dipl.-Ing., M.Sc., and Ph.D. degrees in electrical engineering from the University of Belgrade, Belgrade, Serbia, in 1988, 1993, and 1997, respectively. He is a Professor of energy systems and networks with Newcastle University, U.K. He is also a Distinguished Visiting Professor with Shandong University, China; and a Guest Professor with the Technical University of Munich, Germany. From 2021 to 2022, he was a Full Professor with Skoltech, Russian Federation. From 2006 to 2020, he was the EPSRC Chair Professor with The University of Manchester, U.K. From 2000 to 2006, he was a Senior Specialist of switchgear and distribution automation with ABB, Ratingen, Germany. From 1997 to 1999, he was an Associate Professor with the University of Belgrade. His current research interests include smart grid applications, wide-area monitoring, protection and control, multi-energy systems, switchgear and transient processes, ICT, data analytics, and DSP applications in power systems. He is as Humboldt Fellow. He was a recipient of the National Friendship Award, China. He is the Editor-in-Chief of the *International Journal of Electrical Power and Energy Systems*.